Surface imaging of inelastic Friedel oscillations

J. Fransson[1,2,*] and A. V. Balatsky[1,3,†]

[1]*Theoretical Division, Los Alamos National Laboratory, Los Alamos, New Mexico 87545, USA*

[2]*Center for Nonlinear Studies, Los Alamos National Laboratory, Los Alamos, New Mexico 87545, USA*

[3]*Center for Integrated Nanotechnologies, Los Alamos National Laboratory, Los Alamos, New Mexico 87545, USA*

(Received 24 January 2007; revised manuscript received 29 March 2007; published 24 May 2007)

Impurities that are present on the surface of a metal often have internal degrees of freedom. Inelastic scattering due to impurities can be revealed by observing local features seen in the tunneling current with a scanning tunneling microscope (STM). We consider localized vibrational modes coupled to the electronic structure of a surface. We argue that vibrational modes of impurities produce Fermi momentum k_F oscillations in second derivative of current with respect to voltage $\partial^2 I(\mathbf{r},V)/\partial V^2$. These oscillations are similar to the well-known Friedel oscillations of screening charge on the surface. We propose to measure inelastic scattering generated by the presence of the vibrational modes with STM by imaging the $\partial^2 I/\partial V^2$ oscillations on the metal surface.

DOI: 10.1103/PhysRevB.75.195337 PACS number(s): 68.37.Ef, 72.10.Di

I. INTRODUCTION

Inelastic electron tunneling spectroscopy (IETS) with scanning tunneling microscope, IETS-STM, is a well-established technique, starting with an important experiment by Stipe *et al.*[1] These experiments show steplike features in the tunneling current and local density of states (DOS). The physical explanation of the effect is straightforward: once the energy of the tunneling electron exceeds the energy required to excite local vibrations, there is a new scattering process that contributes to the scattering of electrons due to inelastic excitation of the local mode.[2] The local vibrational modes can be seen in differential conductance measurements as sidebands to the main (elastic) conductance peak.[3] Recently, IETS-STM was used to measure the spin excitations of individual magnetic atoms.[4] In addition, recent experiments show dominant inelastic channels which are strongly spatially localized to particular regions of a molecule.[5]

Improvements in spectroscopic and microscopic measurements have provided new information about fundamental aspects of scattering and interactions in the solid state. Recently, STM technique has evolved from imaging of surfaces[6] to spin-polarized tips for magnetic sensitivity of the readout[4] and spin-polarized injection of the tunneling current used in the measurements.[7] STM has also been used to detect Kondo interactions between conduction electrons and single atomic spins[8,9] and to study the properties of individual atoms.[10,11]

We propose to use the resolution of STM to address spatially resolved inelastic tunneling features produced by local inelastic scattering of the molecule both near the scattering center and at far distances. The "fingerprint" of the inelastic scattering will be present even away from the scattering center. Using local IETS-STM would enable measurements of the standing waves produced by inelastic scattering off impurities, which could be revealed as waves seen in the *second derivative* $\partial^2 I(\mathbf{r},V)/\partial V^2$. For the simplest model of parabolic conduction band, these waves will be seen as standing waves with period set by the Fermi momentum k_F. These standing waves are seen in the oscillations of the $\partial^2 I(\mathbf{r},V)/\partial V^2$ and are *similar but qualitatively different* from the conventional Friedel oscillations.

In case of regular Friedel oscillations, the charge that screens off the impurity exhibit oscillations at large distances from the impurity.[12] Recent STM measurements have observed standing-wave patterns in the elastic-scattering channels on surfaces with atomic impurities adsorbed on the surface,[13,14] sometimes referred to as energy-resolved Friedel oscillations and is the modulated local DOS formed by scattering and interference in the surface electron gas. These oscillations are seen in a wide range of bias as they reflect screening of the charge by electron states in the whole bandwidth. Inelastic scattering of surface electrons off the molecules may be viewed as *inelastic* Friedel oscillations produced by the electron states that are involved in screening. Inelastic Friedel oscillations are seen only in the narrow window of energies near the energy of the mode ω_0 at which inelastic scattering occurs, in contrast to conventional Friedel screening. The possibility of measuring remote response from inelastic scattering in quantum corrals was also briefly discussed by Manoharan *et al.*[15] and Gadzuk and Plihal.[16]

It was recently proposed to use IETS-STM to address the inelastic-scattering features in the Bi2212 superconductors.[17,18] In the case of superconductors, the situation is more involved since one has to deal with the more complicated band structure of Bi2212 and with the inelastic scattering off the distributed bosonic modes. The work presented here allows one to test similar ideas in a more controlled set up where the metal surface and molecular modes are well understood.

The paper is organized as follows. In Sec. II we introduce a model which describes the addressed issue, and some numerical results are discussed in Sec. III. The paper is concluded in Sec. IV.

II. PROBING THE FRIEDEL OSCILLATIONS AND INELASTIC-SCATTERING MEASUREMENTS

The system we consider consists of a two-dimensional surface on which inelastic-scattering centers are randomly distributed. For simplicity, we assume that the impurities are distributed sufficiently far from each other so that their mutual interactions can be neglected. All vibrational modes have energy ω_0 and are assumed to be the same as they would come from the same type of molecules. We use the Hamiltonian for the local vibrational modes, coupled to electrons via Holstein coupling[19] with interactions assumed to occur only at the single impurity site, so that

$$\mathcal{H} = \sum_{\mathbf{k}\sigma} \varepsilon_{\mathbf{k}} c^\dagger_{\mathbf{k}\sigma} c_{\mathbf{k}\sigma} + \omega_0 b^\dagger b + \lambda \sum_{\mathbf{k}\mathbf{k}'\sigma} c^\dagger_{\mathbf{k}\sigma} c_{\mathbf{k}'\sigma}(b^\dagger + b). \quad (1)$$

Here, a surface electron is created (annihilated) by $c^\dagger_{\mathbf{k}\sigma}$ ($c_{\mathbf{k}\sigma}$) at the energy $\varepsilon_{\mathbf{k}}$. The strength of the electron-phonon interaction is given by the parameter λ, whereas ω_0 is the mode of the bare phonon which is created (annihilated) by $b^\dagger$ (b). We assume the classical Holstein coupling between the electronic degrees of freedom and local vibrational mode. The coupling strength λ depends on the strength of the dipole coupling between the atomic displacements due to vibrational mode and the local electronic charge density. We will treat this parameter as a phenomenological parameter that can be extracted from the measured $\partial^2 I/\partial V^2$.

The features we are considering should be seen in the second derivative of the tunneling current with respect to the bias voltage V in real space, i.e., $\partial^2 I(\mathbf{r},V)/\partial V^2$. This quantity is directly proportional to the frequency derivative of the local DOS. In second-order perturbation theory, this amounts to taking the frequency derivative of the correction to the density of states, $\delta N(\mathbf{r},\omega)$, due to the influence of the impurity scattering. The real-space electron Green function (GF) is given by

$$G(\mathbf{r},\mathbf{r}';\omega) = G_0(\mathbf{r},\mathbf{r}';\omega) + G_0(\mathbf{r},0;\omega)\Sigma(\omega)G_0(0,\mathbf{r}';\omega), \quad (2)$$

with the zero GF in two spatial dimensions

$$\begin{aligned} G_0(\mathbf{r},\mathbf{r}';\omega) &= \sum_{\mathbf{k}} G_0(\mathbf{k};\omega) e^{i\mathbf{k}\cdot(\mathbf{r}-\mathbf{r}')} \\ &= 2\pi \frac{m}{\hbar^2} J_0(k_F|\mathbf{r}-\mathbf{r}'|)\left(\log\left|\frac{\omega + D}{\omega - D}\right| - i\pi\right). \end{aligned} \quad (3)$$

Here, the bare electron Fourier-transformed GF $G_0(\mathbf{k},\omega) = 1/(i\omega - \varepsilon_{\mathbf{k}})$, whereas $J_0(x)$ is the zeroth-order Bessel function and D is the bandwidth of the substrate electrons. Using standard procedure for frequency summation, the self-energy $\Sigma(\omega)$ is found as

$$\begin{aligned} \Sigma(i\omega) &= -\frac{\lambda^2}{\beta}\sum_{\mathbf{k},m} G_0(\mathbf{k}, i\omega + i\Omega_m) D_0(i\Omega_m) \\ &= \lambda^2 \sum_{\mathbf{k}} \left\{ \frac{n_B(\omega_0) + f(\varepsilon_{\mathbf{k}})}{i\omega + \omega_0 - \varepsilon_{\mathbf{k}}} + \frac{n_B(\omega_0) + 1 - f(\varepsilon_{\mathbf{k}})}{i\omega - \omega_0 - \varepsilon_{\mathbf{k}}} \right\}, \end{aligned} \quad (4)$$

where $D_0(i\omega) = 2\omega_0/(\omega^2 - \omega_0^2)$ is the bare phonon GFs, whereas $n_B(x)$ and $f(x)$ are the Bose and Fermi functions, respectively.

Due to these definitions, it is clear that the correction to the local DOS is given by

$$\delta N(\mathbf{r},\omega) = \frac{1}{\pi} \operatorname{Im} G_0(\mathbf{r},0,\omega)\Sigma(\omega)G_0(0,\mathbf{r},\omega). \quad (5)$$

Since the effects from inelastic scattering are included in the self-energy, we evaluate $\partial \delta N(\omega)/\partial\omega$, which is directly proportional to $\partial^2 I(\mathbf{r},V)/\partial V^2$.

The sharp feature in the self-energy $\operatorname{Im}\Sigma(\omega)$ is connected to the inelastic-scattering feature. Noting that $\operatorname{Re} G_0(\mathbf{r},\mathbf{r}',\omega) \approx 0$, our calculations simplify to $\delta N(\mathbf{r},\omega) \approx (1/\pi) G_0(\mathbf{r},0;\omega)[\operatorname{Im}\Sigma(\omega)]G_0(0,\mathbf{r};\omega)$. We thus find that

$$\delta N(\mathbf{r},\omega) \approx -\pi^3 \left(\frac{2m}{\hbar^2}\right)^2 J_0^2(k_F r) \operatorname{Im}\Sigma(\omega). \quad (6)$$

Analytical continuation, e.g., $i\omega \to \omega + i0^+$, of the self-energy in Eq. (4) gives the imaginary part

$$\operatorname{Im}\Sigma(\omega) = -2\pi^2\lambda^2 \frac{m}{\hbar^2}[2n_B(\omega_0) + 1 + f(\omega + \omega_0) - f(\omega - \omega_0)]. \quad (7)$$

The correction to the local DOS provides the oscillation in real space. The electron-phonon interaction gives rise to an increased local DOS for frequencies $|\omega| > \omega_0$. Assuming the coupling constant in dimensional units given by $\lambda^2 N_0^2 \sim 0.1$, where N_0 is the unperturbed local DOS, we can estimate the magnitude of the correction in the $\partial I/\partial V$ to be on the order of a few percent of background $\partial I/\partial V$.

We find that $\partial^2 I(\mathbf{r},V)/\partial V^2$ is proportional to

$$\frac{\partial}{\partial\omega}\delta N(\mathbf{r},\omega) \approx -\pi^3\left(\frac{2m}{\hbar^2}\right)^2 J_0^2(k_F r)\frac{\partial}{\partial\omega}\operatorname{Im}\Sigma(\omega), \quad (8)$$

where

$$\begin{aligned} \frac{\partial}{\partial\omega}\operatorname{Im}\Sigma(\omega) = 2\pi^2\lambda^2 \frac{m}{\hbar}\frac{\beta}{4}\bigg[&\cosh^{-2}\frac{\beta}{2}(\omega + \omega_0) \\ &- \cosh^{-2}\frac{\beta}{2}(\omega - \omega_0)\bigg]. \end{aligned} \quad (9)$$

Taking $(\beta/4)\cos^{-2}\beta(\omega \pm \omega_0)/2 \to \delta(\omega \pm \omega_0)$, as $T \to 0$, we expect to find sharp features in $\partial^2 I(\mathbf{r},V)/\partial V^2$ around $\omega = \pm\omega_0$ for low temperatures. Hence, our simplified analytical calculations show that inelastic impurities that couple to the surface electrons give rise to Friedel oscillations in the real-space image of $\partial^2 I(\mathbf{r},V)/\partial V^2$.

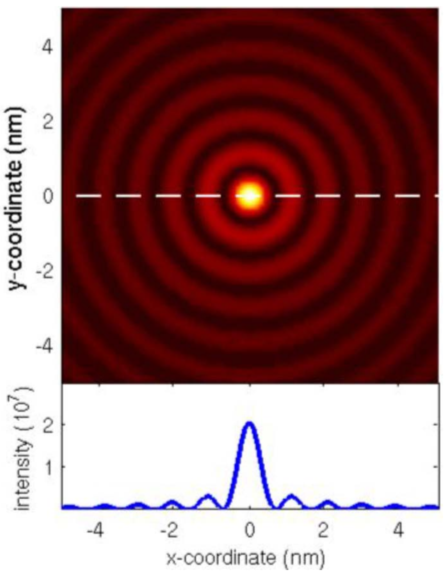

FIG. 1. (Color online) Spatial dependence of $\delta N(\mathbf{r}-\mathbf{r}_0,\omega=\omega_0)$, for $\omega_0=5$ meV, $E_F \simeq 0.45$ eV, and $T=10$ K.

One important point that we also need to address is the role of the dephasing in the inelastic-scattering process. We are dealing with the inelastic-scattering process in which the incoming and outgoing electron waves have different energies. Energy transferred to and/or from the inelastic center implies that the phase change and, hence, the interference of the incoming and outgoing waves will be affected by dephasing caused by scattering. This dephasing process would occur even at $T=0$ and, hence, has nothing to do with the thermal scattering. In the limit of small boson energy $\hbar\omega_0 \ll E_F$, dephasing is small and is not going to destroy the interference of the incoming and outgoing waves. Qualitatively, we can estimate the change in the phase as a result of inelastic scattering as $\delta\phi=\delta\epsilon\delta t$. Here, $\delta\epsilon=\hbar\omega_0$ is the energy transferred to and/or from the electron and $\delta t \sim a/v_F$ is the typical time for the collision of electron with the impurity of size a, assumed to be on the unit-cell size. Then we estimate $a=2\pi/k_F$ and obtain

$$\delta\phi \sim 2\pi\hbar\omega_0/E_F \ll 2\pi. \tag{10}$$

Therefore the interference between incoming and outgoing waves will survive as long as energy transferred in the collision is small.

III. RESULTS

Although the analytical calculations in Sec. II clearly show the oscillatory response of the inelastic scattering, we provide in this section some numerical results to emphasize our proposal. The numerical calculations of $\delta N(\mathbf{r},\omega)$ are based on the full expression presented in the Appendix.

From Eq. (8), it is clear that the oscillations only have a radial component, because the assumed electron-phonon coupling is rotationally invariant. This feature is manifested in Fig. 1, where the upper panel shows the spatial dependence of $\delta N(\mathbf{r}-\mathbf{r}_0,\omega_0)$ at the resonance energy $\omega=\omega_0$. The lower panel shows the intensity of $\delta N(x-x_0,0;\omega_0)$, on the line $\mathbf{r}-\mathbf{r}_0=x-x_0$, which corresponds to the dashed line in the upper panel. The features in $\delta N(\mathbf{r}-\mathbf{r}_0,\omega)$ depend on the spatial position *and* on the frequency. In Fig. 2, which shows a contour plot of $\delta N(x-x_0,0;\omega)$, we illustrate the fact that the inelastic Friedel oscillations occur in a narrow interval around $\omega=\pm\omega_0$. The plot clearly illustrates that there is hardly any intensity at all for frequencies off the phonon mode ω_0. The plot in Fig. 3 illustrates the IETS-STM resonance signal on a surface with four independent inelastic-scattering centers, analogous to the plot in Fig. 1. As expected from the wave character of the signal, the pattern on the surface is because of interfering Friedel oscillations from the four scattering centers. This interference appearing in the plot is due to the sum of waves with coherent phases. The coherent waves are generated at the four independent scattering centers.

Next suppose that the position of the STM tip is kept fixed in space, i.e., letting $\mathbf{r}-\mathbf{r}_0=0$, where $\mathbf{r}_0$ is the position of the inelastic-scattering center. Then, as shown in the previous section, the derivative $\partial\delta N(0,\omega)/\partial\omega$ is expected to peak or dip at $\omega=\pm\omega_0$, cf Eqs. (8) and (9), as the fre-

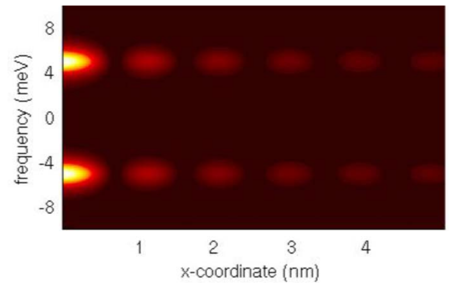

FIG. 2. (Color online) Spatial and frequency dependences of $|\partial\delta N(\mathbf{r},\omega)/\partial\omega|$ at $T=5$ K. Other parameters as in Fig. 1.

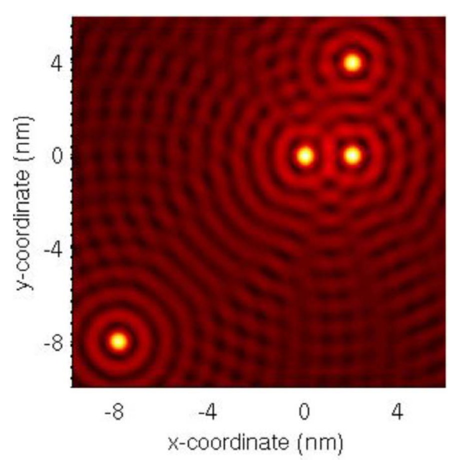

FIG. 3. (Color online) Calculated IETS-STM resonance, e.g., at phonon mode resonance, sum of the signal on surface with four noninteracting inelastic impurities embedded. The interference appearing in the plot is due to the sum of waves with coherent phases. The coherent waves are generated at the four independent scattering centers. For parameters used, see Fig. 1.

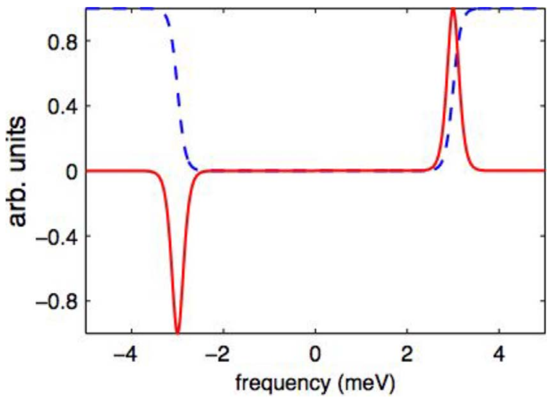

FIG. 4. (Color online) $\partial \delta N(0,\omega)/\partial\omega$ (solid) and $\delta N(0,\omega)$ (dashed) for $\omega_0=3$ meV and $T=1$ K. Other parameters as in Fig. 1.

quency is varied. This is illustrated in Fig. 4 (solid). These local extrema correspond to steps in $\delta N(0,\omega)$, which is also clear in Fig. 4 (dashed).

From Eq. (9) we find that the intensity of the peaks in $|\partial\delta N/\partial\omega|$ is highly temperature dependent, which is illustrated in Fig. 5 for two temperatures. The plots clearly show that the peaks become sharper for decreasing temperatures, illustrating the δ-function-like behavior at low temperatures.

IV. CONCLUSIONS

We propose a scanning technique that allows one to visualize the oscillations in the inelastic scattering produced by the local modes. The standard way to image IETS of the molecule is to measure $\partial^2 I(\mathbf{r},V)/\partial V^2$ locally near the scattering center.[1,4,5] We point out that the fingerprint of the inelastic scattering will be present even away from the scattering center. The incoming electron wave donates and/or absorbs energy from the inelastic-scattering center. In the process of inelastic scattering, the incoming and outgoing electron waves interfere. This interference can be clearly seen in the real-space oscillations of the second derivative $\partial^2 I(\mathbf{r},V)/\partial V^2$ with characteristic momentum k_F. The important point is that for the flat density of states the interference between states that have undergone inelastic scattering will only be present at the bias $eV=\hbar\omega_0$ and not at other energies. This makes the proposed effect very different from the conventional Friedel oscillations that occur for elastic scattering and are present for the wide range of energies as the whole band of electrons participates in screening. We also argue that as long as the energy difference between these states is small compared with the Fermi energy of electrons, the dephasing in the process of scattering is small and hence interference is preserved.

The technique, proposed here, can be applied to the inelastic scattering of the electrons from the local vibrational modes of the molecules on the surface[5] and would offer exciting possibilities to image the interference and interactions between inelastic-scattering processes in the ensemble of few scattering centers.

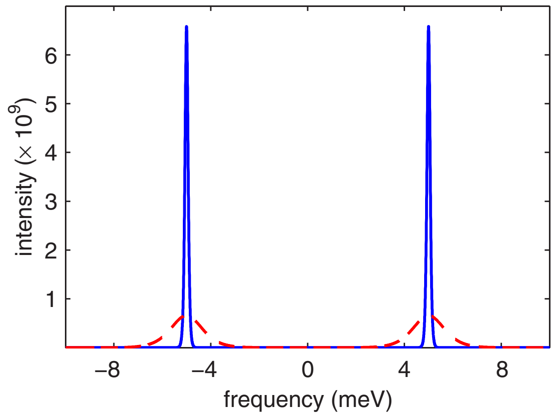

FIG. 5. (Color online) The derivative ($|\partial\delta N/\partial\omega|$) for different temperatures $T\in\{0.01,0.1\}$ K {solid, dashed}. The plots have been artificially broadened. Other parameters as in Fig. 1.

In our analysis of the IETS effect we made few simplifying assumptions. We took the GFs in our calculations to be at Fermi energy. If we retain energy dependence of the GFs used in our calculation, the $J_0(k_F r)$ should be replaced by $J_0(kr)$, with momentum k determined by the true energy of the particle. We also assumed the band structure local DOS to be flat so we can emphasize the IETS effect due to molecule scattering. The $\partial I/\partial V$ in realistic setup will have energy dependence due to *nonflat* DOS as a function of energy. Moreover, for the real band structure of the surface of the metal even on the pristine surface, $\partial I/\partial V$ as a function of position will exhibit modulations that occur due to atomic modulations. All these assumptions are not critical and were made to make calculation as transparent as possible to elucidate the nature of the IETS oscillations *off molecule* that might be measured by STM. Combined real-space and energy dependences of the underlying $\partial I/\partial V$ will produce the background features in $\partial^2 I/\partial V^2$ even before we "turn on" the inelastic scattering off a single molecule. The theoretical and experimental challenge is to be able to separate these background effects from the IETS features due to molecule scattering.

ACKNOWLEDGMENTS

This work has been supported by US DOE, LDRD, and BES, and was carried out under the auspices of the NNSA of the US DOE at LANL under Contract No. DE-AC52-06NA25396. We are grateful to M. Crommie, J. C. Davis, D. Eigler, W. Harrison, H. Manoharan, and R. Wiesendanger for useful discussions.

APPENDIX: DERIVATION OF δN

In the above analysis, we neglected the real part of the unperturbed Green's functions. However, as we show here, taking this part into account does not significantly change the picture. We have

$$\delta N(\mathbf{r},\omega) = -\frac{1}{\pi}\left(\frac{2\pi m}{\hbar^2}\right)^2 J_0^2(k_F r)\left\{\pi^2 \,\mathrm{Im}\,\Sigma(\omega) - \left[\mathrm{Im}\,\Sigma(\omega)\log\left|\frac{\omega+D}{\omega-D}\right| - 2\pi\,\mathrm{Re}\,\Sigma(\omega)\right]\log\left|\frac{\omega+D}{\omega-D}\right|\right\}.$$

Since we are interested in the frequency derivative of this expression, we find that

$$\frac{\partial}{\partial\omega}\delta N(\mathbf{r},\omega) = -\frac{1}{\pi}\left(\frac{2\pi m}{\hbar^2}\right)^2 J_0^2(k_F r)\left\{\pi^2\frac{\partial}{\partial\omega}\,\mathrm{Im}\,\Sigma(\omega) - \left[\frac{\partial}{\partial\omega}\,\mathrm{Im}\,\Sigma(\omega)\right]\log\left|\frac{\omega+D}{\omega-D}\right| + \mathrm{Im}\,\Sigma(\omega)\frac{4D}{\omega^2-D^2}\log\left|\frac{\omega+D}{\omega-D}\right| + 2\pi\left[\frac{\partial}{\partial\omega}\,\mathrm{Re}\,\Sigma(\omega)\right]\log\left|\frac{\omega+D}{\omega-D}\right| - 2\pi\,\mathrm{Re}\,\Sigma(\omega)\frac{2D}{\omega^2-D^2}\right\}.$$

Here,

$$\mathrm{Re}\,\Sigma(\omega) = 2\pi\lambda^2\frac{m}{\hbar^2}\int\left\{\frac{n_B(\omega_0)+f(\varepsilon)}{\omega+\omega_0-\varepsilon} + \frac{n_B(\omega_0)+1-f(\varepsilon)}{\omega-\omega_0-\varepsilon}\right\}d\varepsilon$$
$$= 2\pi\lambda^2\frac{m}{\hbar^2}\left\{n_B(\omega_0)\log\left|\frac{\omega+\omega_0+D}{\omega+\omega_0-D}\right| + [n_B(\omega_0)+1]\log\left|\frac{\omega-\omega_0+D}{\omega-\omega_0-D}\right| - 2\omega_0\int\frac{f(\varepsilon)}{(\omega-\varepsilon)^2-\omega_0^2}d\varepsilon\right\},$$

which gives the derivative

$$\frac{\partial}{\partial\omega}\,\mathrm{Re}\,\Sigma(\omega) = -2\pi\lambda^2\frac{m}{\hbar^2}\int\left\{\frac{n_B(\omega_0)+f(\varepsilon)}{(\omega+\omega_0-\varepsilon)^2} + \frac{n_B(\omega_0)+1-f(\varepsilon)}{(\omega-\omega_0-\varepsilon)^2}\right\}d\varepsilon$$
$$= 4\pi\lambda^2\frac{m}{\hbar^2}\left\{D\frac{n_B(\omega)}{(\omega+\omega_0)^2-D^2} + D\frac{n_B(\omega_0)+1}{(\omega-\omega_0)^2-D^2} + 2\omega_0\int f(\varepsilon)\frac{\omega-\varepsilon}{[(\omega-\varepsilon)^2-\omega_0^2]^2}d\varepsilon\right\}.$$

However, since the logarithm $\log|(\omega\pm\omega_0+D)/(\omega\pm\omega_0-D)|\approx 0$ for $D\gg|\omega\pm\omega_0|$, we see that all terms but the first are negligible in $\partial\delta N/\partial\omega$.

*Electronic address: jonasf@lanl.gov
†Electronic address: avb@lanl.gov

[1] B. C. Stipe, M. A. Rezaei, and W. Ho, Science **280**, 1732 (1998).
[2] R. C. Jaklevich and J. Lambe, Phys. Rev. Lett. **17**, 1139 (1966); J. Lambe and R. C. Jaklevich, Phys. Rev. **165**, 821 (1968).
[3] H. Park, J. Park, A. K. L. Lim, E. H. Anderson, A. P. Alivisatos, and P. L. McEuen, Nature (London) **407**, 57 (2000).
[4] A. J. Heinrich, J. A. Gupta, C. P. Lutz, and D. M. Eigler, Science **306**, 466 (2004); C. F. Hirjibehedin, C. P. Lutz, and A. J. Heinrich, *ibid.* **312**, 1021 (2006).
[5] M. Grobis, K. H. Khoo, R. Yamachika, X. Lu, K. Nagaoka, S. G. Louie, M. F. Crommie, H. Kato, and H. Shinohara, Phys. Rev. Lett. **94**, 136802 (2005).
[6] G. Binnig and H. Rohrer, Rev. Mod. Phys. **59**, 615 (1987).
[7] S. Heinze, M. Bode, A. Kubetzka, O. Pietzsch, X. Nie, S. Blügel, and R. Wiesendanger, Science **288**, 1805 (2000); A. Kubetzka, M. Bode, O. Pietzsch, and R. Wiesendanger, Phys. Rev. Lett. **88**, 057201 (2002); A. Wachowiak, J. Wiebe, M. Bode, O. Pietzsch, M. Morgenstern, and R. Wiesendanger, Science **298**, 577 (2002); J. Wiebe, A. Wachowiak, F. Meier, D. Haude, T. Foster, M. Morgenstern, and R. Wiesendanger, Rev. Sci. Instrum. **75**, 4871 (2004).
[8] V. Madhavan, W. Chen, T. Jamneala, M. F. Crommie, and N. S. Wingreen, Science **280**, 567 (1998); Phys. Rev. B **64**, 165412 (2001).
[9] J. Li, W.-D. Schneider, R. Berndt, and B. Delley, Phys. Rev. Lett. **80**, 2893 (1998).
[10] A. Yamasaki, W. Wulfhekel, R. Hertel, S. Suga, and J. Kirschner, Phys. Rev. Lett. **91**, 127201 (2003).
[11] M. Bode, O. Pietzsch, A. Kubetzka, and R. Wiesendanger, Phys. Rev. Lett. **92**, 067201 (2004).
[12] J. Friedel, Nuovo Cimento, Suppl. **7**, 287 (1958).
[13] Y. Hasegawa and Ph. Avouris, Phys. Rev. Lett. **71**, 1071 (1993).
[14] M. F. Crommie, C. P. Lutz, and D. M. Eigler, Nature (London) **363**, 524 (1993).
[15] H. C. Manoharan, C. P. Lutz, and D. M. Eigler, Nature (London) **403**, 512 (2000).
[16] J. W. Gadzuk and M. Plihal, Phys. Rev. B **68**, 235413 (2003).
[17] J.-X. Zhu, A. V. Balatsky, T. P. Devereaux, Q. Si, J. Lee, K. McElroy, and J. C. Davis, Phys. Rev. B **73**, 014511 (2006).
[18] A. V. Balatsky, I. Vekhter, and J.-X. Zhu, Rev. Mod. Phys. **78**, 373 (2006).
[19] T. Holstein, Ann. Phys. (N.Y.) **8**, 325 (1959).